



저작자표시-비영리-변경금지 2.0 대한민국

이용자는 아래의 조건을 따르는 경우에 한하여 자유롭게

- 이 저작물을 복제, 배포, 전송, 전시, 공연 및 방송할 수 있습니다.

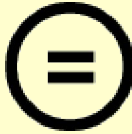
다음과 같은 조건을 따라야 합니다:



저작자표시. 귀하는 원저작자를 표시하여야 합니다.



비영리. 귀하는 이 저작물을 영리 목적으로 이용할 수 없습니다.



변경금지. 귀하는 이 저작물을 개작, 변형 또는 가공할 수 없습니다.

- 귀하는, 이 저작물의 재이용이나 배포의 경우, 이 저작물에 적용된 이용허락조건을 명확하게 나타내어야 합니다.
- 저작권자로부터 별도의 허가를 받으면 이러한 조건들은 적용되지 않습니다.

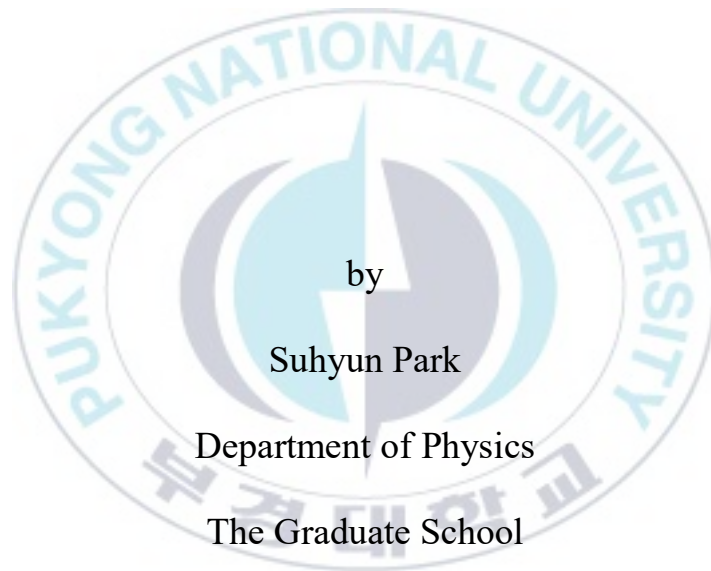
저작권법에 따른 이용자의 권리는 위의 내용에 의하여 영향을 받지 않습니다.

이것은 [이용허락규약\(Legal Code\)](#)을 이해하기 쉽게 요약한 것입니다.

[Disclaimer](#)

Thesis for the Degree of Master of Physics

A study on Imatinib Binding Associated with Sequential
Conformational Change of c-Src Tyrosine Kinase to
Imatinib Revealed by Molecular Dynamics Simulation



by

Suhyun Park

Department of Physics

The Graduate School

Pukyong National University

August 2020

A study on Imatinib Binding Associated with Sequential Conformational
Change of c-Src Tyrosine Kinase to Imatinib Revealed by Molecular
Dynamics Simulation

분자 동역학 시뮬레이션을 통한 c-Src 티로신 키나아제의 순
차적인 구조 변화에 따른 이마티닙 결합에 대한 연구

Advisor: Prof. Sangwook Wu

by

Suhyun Park

A thesis submitted in partial fulfillment of the requirements
for the degree of

Master of Physics

in Department of Physics, The Graduate School,
Pukyong National University

August 2020

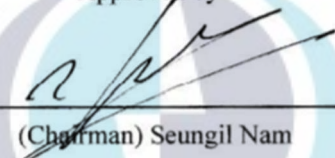
A study on Imatinib Binding Associated with Sequential Conformational
Change of c-Src Tyrosine Kinase to Imatinib Revealed by Molecular
Dynamics Simulation

A dissertation

by

Suhyun Park

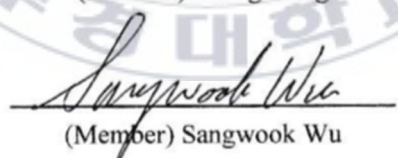
Approved by



(Chairman) Seungil Nam



(Member) Jisang Hong



(Member) Sangwook Wu

August 2020

Contents

I. Introduction	1
1. Tyrosine Kinase	1
1.1. Protein tyrosine kinases (PTKs)	2
1.2. Src Family Kinase (SFKs)	3
1.3. Organization and structure of c-Src tyrosine kinase	4
1.4. Tyrosine kinase inhibitor (TKI)	8
2. Docking	9
2.1. Docking mechanism	9
II. Methods	11
1. Molecular Dynamics Simulation (MD simulation)	11
1.1. Molecular mechanic force filed	12
1.2. Targeted Molecular Dynamics Simulation	21
2. Molecular docking	22
2.1. Autodock	23
2.2. Swissdock	25
III. Results and Discussion	26
IV. Conclusions	36
Reference	37

List of Figures

Figure I- 1 . Domain structure of c-Src tyrosine kinase. The Src family kinase consisted of common domain constructs. SH: homology domain.....	4
Figure I- 2 . Two X-ray crystal structures of the c-Src tyrosine kinase: Inactive conformation (PDB id : 2SRC) and active conformation (PDB id : 1Y57).	5
Figure I- 3 . Inactive conformation of c-Src Tyrosine kinase and biologically important regions (Linker, Activation loop, C-terminal tail, and C-Helix).	7
Figure I- 4 . Active conformation of c-Src Tyrosine kinase and biologically important regions (Linker, Activation loop, C-terminal tail, and C-Helix).	7
Figure I- 5 . Chemical structure of Imatinib.....	8
Figure I- 6 . Look-and-Key model and Induced-Fit model.....	10
Figure II- 1 . Schematic representation of the four components to a molecular mechanics force field: bond stretching, angle bending, torsional terms and non-bonded interactions.	14
Figure II- 2 . Comparison of the Morse potential (black, solid line) and harmonic oscillator potential (blue, dotted line).	15
Figure II- 3 . Periodic boundary conditions in two dimensions. The length of box is L.	18
Figure II- 4 . Geometry of the conformational transition from $\mathbf{x}i$ to $\mathbf{x}F$. The r -axis is chosen in such a way that the initial configuration defines the origin and the final configuration lies on the positive branch. $\mathbf{S}i$ is one of the residual Cartesian coordinates. A TMD simulation run generates	

configuration $\mathbf{x}(t)$ lying on hyperspheres with radius $\rho(t)$ centered in $\mathbf{x}F$. The quasicontinuous contraction of the hypersphere from a radius ρ_0 to ρ_f enforces the conformational transition.[33].....22

Figure III- 1 . Six Snapshots of TMD trajectory during 10 ns. (A) 0ns : Starting structure (Inactive conformation). (B) 2 ns, (C) 4 ns, (D) 6 ns, (E) 8 ns, (F) 10 ns : Targeting structure (Active conformation). In particular, the protein structure (F) exactly matches the active state protein crystal structure.....27

Figure III- 2 . At this time, Imatinib moves dynamically without being fixed according to a given torsion when it is docked. The gridbox of Autodock is set to (60*60*60Å³).....28

Figure III- 3 . 2ns structure created by MD simulation. Docking images of Imatinib to a c-Src tyrosine kinase are generated by AUTODOCK (blue) and SWISSDOCK (pink).....29

Figure III- 4 . 4ns structure created by MD simulation. Docking images of Imatinib to a c-Src tyrosine kinase are generated by AUTODOCK (blue) and SWISSDOCK (pink).....30

Figure III- 5 . 6ns structure created by MD simulation. Docking images of Imatinib to a c-Src tyrosine kinase are generated by AUTODOCK (blue) and SWISSDOCK (pink).....31

Figure III- 6 . 8ns structure created by MD simulation. Docking images of Imatinib to a c-Src tyrosine kinase are generated by AUTODOCK (blue) and SWISSDOCK (pink).....32

Figure III- 7 . 10ns structure created by MD simulation. Docking images of Imatinib to a c-Src tyrosine kinase are generated by AUTODOCK (blue) and SWISSDOCK (pink).....33

Figure III- 8 . Gibbs Free Energy for binding of imatinib to various c-Src tyrosine kinase conformations. The arrow denotes the most stable conformation of c-Src tyrosine kinase binding to imatinib.34

Figure III- 9 . Relative conformation of imatinib with DFG (Asp(404)-Phe(405)-
Gly(406)conformation of c-Src tyrosine kinase generated by (A) X-ray (B)
SWISSDOCK (C) AUTODOCK.....35

List of Tables

Table I- 1 . Key region and domain residues of c-Src tyrosine kinase.[20] 6

Table III- 1 . Labels for the various different conformations of c-Src tyrosine
kinase generated by targeted MD simulation.....26



분자 동역학 시뮬레이션을 통한 c-Src 티로신 키나아제의 순차적인 구조 변화에 따른 이마티닙 결합에 대한 연구

박 수 현

부경대학교 대학원 물리학과

요약

소분자 키나제 억제제 (small molecule kinase inhibitor)는 신호전달 경로 (signal transduction pathway)를 표적으로 하므로 넓은 의미로는 신호전달경로 억제제라고 한다. tyrosine kinase inhibitor가 표적으로 하는 kinase는 세포 활성의 신호전달 체계나 조절에 있어서 핵심적인 역할을 수행하는 체내 효소 중 하나이다. 이들 중 c-Src tyrosine kinase는 비활성상태에서 활성상태로의 구조 변화를 통해 세포의 신호전달 경로에 관여 함으로서, 세포분화와 성장에 중요한 역할을 하는 단백질이다. 우리는 c-Src tyrosine kinase의 비활성 상태 (PDB: 2SRC)와 활성 상태 (PDB: 1Y57)에서의 X-ray 구조를 targeted molecular dynamics simulation을 통해 단백질 형태의 변화를 관측하고, Abl-tyrosine kinase의 활성 억제에 매우 효과적으로 작용하는 약물인 이마티닙 (imatinib)을 Autodock과 Swissdock을 이용하여

protein-ligand 결합을 관측하였다.

이 연구에서 이마티닙과 타겟 단백질인 c-Src tyrosine kinase의 작용을 분자 수준에서 이해하고, c-Src tyrosine kinase의 구조 변화 과정에서 이마티닙이 어느 상태의 구조에서 최적의 결합을 하는지에 대해 제시하였다. 이는 약물 설계(drug design)에서 약물의 타겟이 되는 단백질의 구조적 동역학(conformational dynamics)이 약물의 결합(binding)과 해리(dissociation)에 매우 중요한 영향을 준다는 것을 의미한다.



I. Introduction

Kinase is one of the enzymes in the body that plays a key role in signaling and regulation of cellular activity. Among them, protein kinase refers to a protein present in the cell or on the cell surface that plays an important role in the cell signaling system involved in cell metabolism, damage response, adaptation, growth and differentiation. Protein kinase is achieved by activating a specific protein or enzyme through phosphorylation to add a phosphate group to the protein. However, because they are specifically involved in cell growth, proliferation, and differentiation, their mutation may cause abnormal growth or proliferation, which is not regulated in the cell, and may cause cancer.[1, 2, 4] By targeting such mutant protein kinase, tyrosine kinase inhibitor effectively acts as a therapeutic agent. In 2001, the US FDA approved imatinib (Gleevec®) as a treatment for Philadelphia-positive chronic myelogenous leukemia, contributing significantly to the treatment of cancer patients. In this paper, we investigate the change of form from inactive state to active state of c-Src tyrosine kinase, and the imatinib that binds to different areas according to the conformational change of c-Src tyrosine kinase.[5, 6]

1. Tyrosine Kinase

Kinase is a phospho-transferase that removes high energy phosphate from ATP and transfers it to the side chain of the substrate protein's serine, threonine, or tyrosine.

Independent of kinase activity, Src itself is a phospho-protein. c-Src has a phosphate group in one or more amino acid side chains through a covalent bond. This means that c-Src acts as a substrate for phosphorylation by protein kinase.[2,3]

Kinase plays a very important role in metabolism, intercellular signaling, protein regulation, cell transport, secretion, and numerous other cellular reaction pathways, most of which are protein kinase.

1.1. Protein tyrosine kinases (PTKs)

Protein kinase changes the function of proteins through phosphorylation in the cell, resulting in various functions. Tyrosine kinase, a type of protein kinase, transmits one phosphate group to tyrosine from the ATP in the cell, 'on' or 'off' the cell function. That is, the binding of tyrosine to a single phosphate group is called an oxidation, which plays an important role in normal cell growth by regulating intracellular signal transduction and cell activity.[1, 2, 4] Tyrosine kinases are classified into two types: receptor tyrosine kinases (RTKs) and non-receptor tyrosine kinases (NRTKs).

Receptors that recognize external stimuli are called receptor tyrosine kinases (RTKs). RTKs are transmembrane glycoproteins that bind a specific ligand to the extracellular part and transmit an activated signal inside the cell.[2, 6] RTKs include epidermal growth receptor (EGFR), platelet-derived growth factor (PDGF), vascular endothelial growth factor (VEGF), fibroblast growth factor (FGF), nerve growth factor (NGF) and platelet-derived growth factor (PDGF).

Non-receptor tyrosine kinases (NRTKs) are enzymes that catalyze the phosphorylation process by moving ATP into the tyrosine residues of proteins in the cytoplasm.[4, 7]

1.2. Src Family Kinase (SFks)

Src, Lyn, Fyn, Lck, Hck, Blk, Yes, Fgr, Frk are all non-receptors and are called Src family kinases (SFk). Among SFks, Src kinase (i.e. Src, Fyn, Yes) acts on cell cycle, cell adhesion, cell migration, proliferation and differentiation, and is expressed overall in cells and tissues. On the other hand, Fgr, Hck, Lck, Blk, etc. are tissue-specific.[8,9]

In 1911, Peyton Rous harvested and studied sarcoma from chicken breast muscles, and discovered cancer-causing Rous sarcoma virus (RSV).[6,10] The RSV gene that promotes sarcoma formation was called Src. The v-Src protein from the RSV genome initially acts as an oncogene of the retrovirus Rous sarcoma virus. In contrast, c-Src is a homologue in normal v-Src cells. Phosphorylation of Tyr527 inhibits kinase activity. v-Src does not contain Tyr527 and c-Src does not.[11, 12, 13]

All Src family kinases (SFk) proteins consist of domains in which each segment is common. It is called the Src homology domain 1,2,3 and 4(SH1, SH2, SH3 and SH4). this sequence answers the puzzle of receptor signaling. In the N-terminal, the SH4 domain exists, and this part is related to the fixation to lipids. After the SH4 domain, there exists a unique domain (50-70 residues), which has various sequences for each member of the SFk protein. The key components of SFk are the SH3, SH2, Kinase (SH1) domain and C-terminal tail. It starts from residue 84. Due to the unstable and low solubility of SFk, only these key components (SH3, SH2, Kinase and C-terminal tail) is X-ray crystallized.[12,13,14,15]

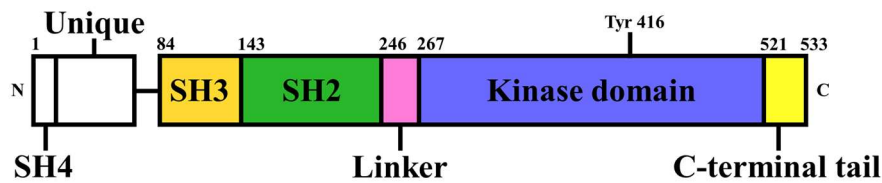


Figure I- 1 . Domain structure of c-Src tyrosine kinase. The Src family kinase consisted of common domain constructs. SH: homology domain.

1.3. Organization and structure of c-Src tyrosine kinase

The conformational transition pathway of c-Src tyrosine kinase key components (SH3, SH2, Kinase and C-terminal tail, residues 84-533) was studied using molecular dynamics simulation.[15,16]

The SH2 domain is a relatively small domain composed of about 100 amino acid residues and acts as a receptor inside the cell. It also helps to bind to a partner protein with an amino acid sequence containing phosphorylated tyrosine, resulting in a physical complex between the two proteins.[17,18]

The SH3 domain consists of compact five β -strands and two prominent loops.[20] This part adopts poly-proline type II helical conformation when creating a complex with the SH3 domain and specifically binds to the proline-rich sequences of partner proteins. The SH3 domain is a very important area involved in intracellular signal transduction by acting alone or in combination with the SH2 domain or modular domain.[17, 18, 19]

In the active state of c-Src, these domains interact with partner proteins. However, in the inactive state, it interacts with the molecule through the proline-rich linker and the C-terminal tail.[20] SH1 and kinase domains are composed of

smaller N-terminal lobe and larger C-terminal lobe.[21] Here, the larger C-terminal lobe mainly composed of α -helix plays an important role in the morphological change of c-Src. In order to change the shape of c-Src, α C helix must be changed, and the important residue is Glu310. Glu310 forms a salt-bridge with Lys295 in the active state to maintain closed conformation. Activation loops performing autophosphorylation at Tyr 416 are N-terminal lobe and C-terminal lobe. It is located in between and is an important part for c-Src shape change.[9,18,21]

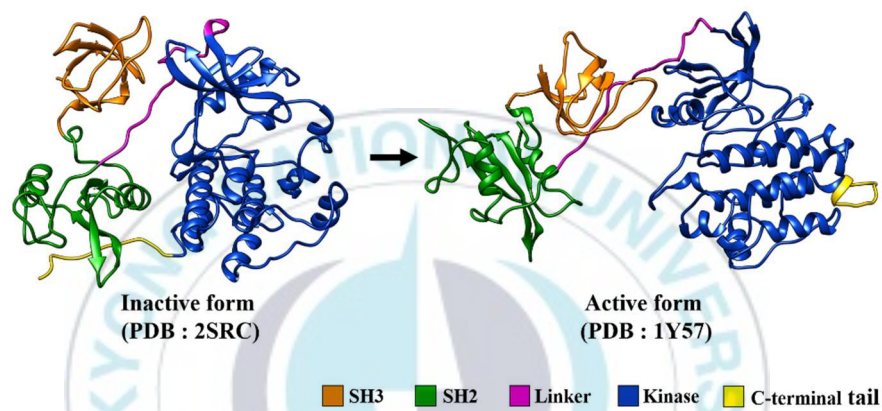


Figure I- 2 . Two X-ray crystal structures of the c-Src tyrosine kinase: Inactive conformation (PDB id : 2SRC) and active conformation (PDB id : 1Y57).

In a normal cellular environment, c-Src tyrosine kinase remains inactive (PDB: 2SRC).[13] When Tyr527 in the SH2 region becomes phosphorylated (pTyr527) and c-Src maintains closed conformation and forms an inactive protein structure. The c-Src tyrosine kinase causes conformational change by external cell signal transduction, and can be changed from an inactive state to an active state (active, PDB: 1Y57).[21] The activation mechanism of c-Src tyrosine kinase is achieved

by controlling phosphorylation. In the inactive state, pTyr527 undergoes dephosphorylation in pTyr527 in the process of transition to the active state, causing a structural change from closed conformation to open conformation, and in this process, Tyr416, which is located near the activation loop, is phosphorylated through autophosphorylation.[18]

Domain	Residue number
SH3 domain	Thr84 - Ser142
SH2 domain	Ile143 - Cys245
Linker	Pro246 - Ser266
Kinase domain	Leu267 - Phe520
C-terminal tail	Thr521 - Leu533
Activation loop	Asp404 - Glu432
α C helix	Pro304 - Lys316

Table I- 1 . Key region and domain residues of c-Src tyrosine kinase.[20]

These various domains transmit signals only to the target protein precisely through highly specialized interactions between proteins inside the cell.[22] Cells can also receive and process biochemical signals that regulate cell proliferation. If there is a problem with c-Src tyrosine kinase signaling problems, cancer develops. To truly understand the complexity of cancer, we have to understand how c-Src tyrosine kinase manages cell proliferation.[23]

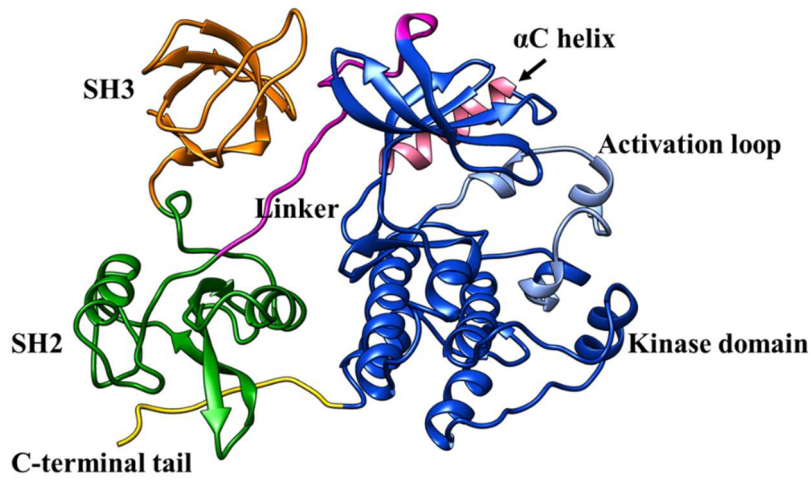


Figure I- 3 . Inactive conformation of c-Src Tyrosine kinase and biologically important regions (Linker, Activation loop, C-terminal tail, and C-Helix).

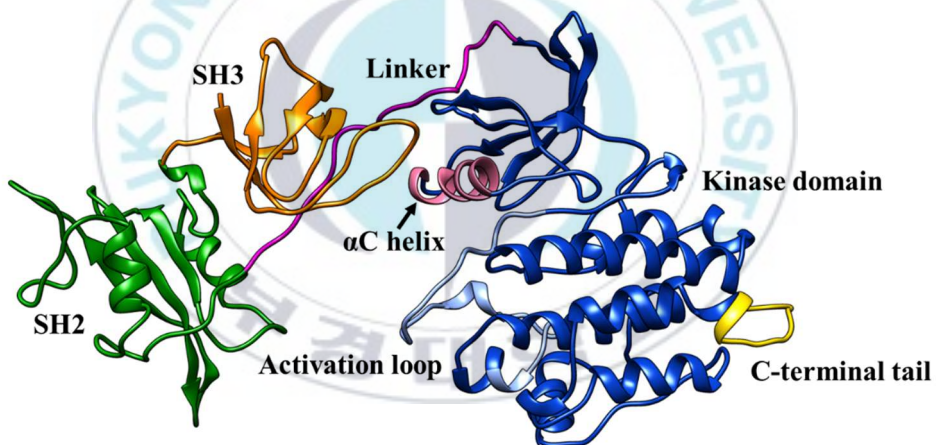


Figure I- 4 . Active conformation of c-Src Tyrosine kinase and biologically important regions (Linker, Activation loop, C-terminal tail, and _C-Helix).

1.4. Tyrosine kinase inhibitor (TKI)

It is known that the growth factor receptor on the cell surface plays a very important role in the growth of cancer cells.[2,6] The signaling pathway inhibitor, which is a targeted therapeutic agent, prevents growth factors from binding to the receptor or blocks the activation of the cancer cells.[22, 23, 24]

Tyrosine kinase is an important component of the signaling pathway in which extracellular ligands carry important information from the cytoplasm to the nucleus. When this receptor is activated abnormally, many types of cancer are caused.[22] Therefore, blocking tyrosine kinase may act as an anticancer agent. The first tyrosine kinase inhibitor, imatinib, is a drug better known under the trade name Gleevec®. Imatinib is a drug that inhibits the activity of tyrosine kinase, expressed by a kind of cancer gene called the Philadelphia gene, produced by fusion by the chromosomal translocation of the Bcr and Abl genes. Tyrosine kinases are known to cause chronic myeloid leukemia (CML). Gleevec® works very well on Abl tyrosine kinases, but it does not appear to have a significant effect on c-Src tyrosine kinases, which have 47% similarity to Abl amino acid sequences.

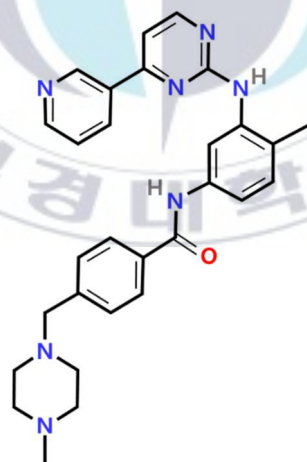


Figure I- 5 . Chemical structure of Imatinib

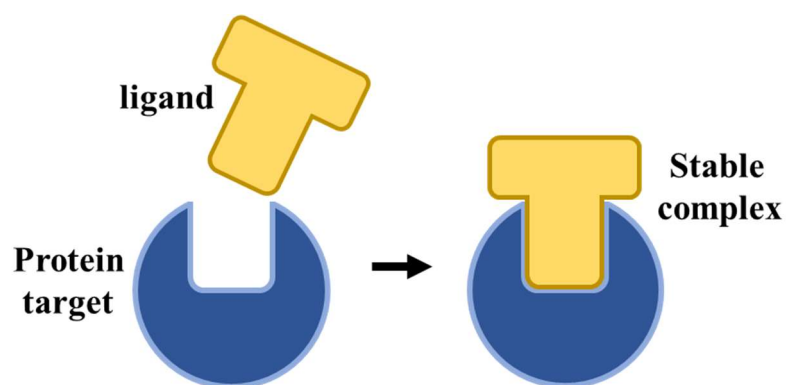
2. Docking

Docking is one of the most commonly used techniques in drug design, and is used to measure the strength of protein-ligand interactions and to identify the correct posture of a ligand at a binding site. This docking suggests that contributes to the study of protein function or further research on drug development that inhibits the function of protein. There are a few things to consider when docking, including protein flexibility, search algorithms, and scoring functions.[25,26]

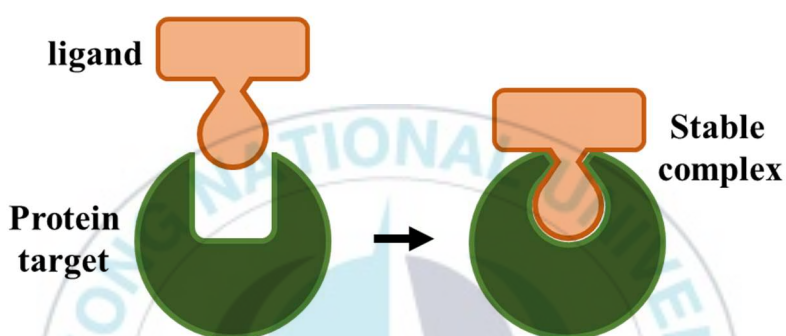
2.1. Docking mechanism

Due to the structural flexibility of proteins and ligands, the active site may change during docking. Molecular docking is defined as an optimization problem, which describes the best-fit orientation of the ligand that binds to the target protein. During docking, the structure where the binding structure between protein and ligand fits like a lock and a key is a 'lock-and-key model'. On the other hand, the case where the structure of protein and ligand changes in order to find the best-fit is called the 'induced-fit model'. [25]

In the induced-fit model, the active site of the protein undergoes morphological changes when exposed to the substrate to improve binding. This can predict a more accurate active position result, but it can also complicate calculations by innumerable variables. Methods to supplement this include soft docking, Rotamer library usage, Monte Carlo simulation, Molecular Dynamics simulation, and Ensemble usage. [27]



Lock-and-Key



Induced-Fit

Figure I-6 . Look-and-Key model and Induced-Fit model.

The flexibility of the ligand as well as the protein should be considered. There are systematic search algorithms that consider all degrees of freedom of the ligand and stochastic search algorithms that consider it as a probability function according to a given structural change. However, in order to evaluate the compatibility between protein-ligands using any calculation method, conformal sampling must be performed through a scoring function (or energy function). When docking is complete, the result is usually selected by scores. The accuracy of the scoring function greatly affects the quality of the docking results. The

scoring function of the docking tool to be used in the experiment is described in Method.

Flexible docking programs include Autodock, Autodock vina,[27] GOLD (Genetic Optimisation for Ligand), FlexX (Flexible docking using an incremental construction algorithm), DOCK, Internal Coordinate Mechanics (ICM), etc., Docking wedserver includes HADDOCK, Swissdock, Zdock and so on.[28]

II. Methods

In this study, two methods are employed Target Molecular dynamics simulation and Molecular docking. Target Molecular dynamics simulation was used to confirm the change of c-Src tyrosine kinase from inactive (PDB ID: 2SRC) to active (PDB ID: 1Y57), and this was performed with MD simulation analysis technique RMSD. Imatinib (Gleevec®) was docked using Autodock and Swissdock for 0ns (inactive state), 2ns, 4ns, 6ns, 8ns, and 10ns (active state) results derived from each simulation result respectively .

1. Molecular Dynamics Simulation (MD simulation)

In this study, the target Molecular Dynamics (TMD) Simulation confirmed the shape change from Inactive (PDB: 2SRC) to Active (PDB:1Y57).[29] To this end, the structure of the starting state and the structure of the target state are configured to have the same number of atoms, and the total number of atoms is 131,476. In TMD simulation, the number of atoms (N) affected by external potential is 3,619 atoms (non-hydrogen heavy atoms) except hydrogen. TMD simulation was

performed at a temperature of 310 K in the TIP3 water model, and the total time of simulation in the NPT ensemble was set to 10 ns. MD simulation for structural changes of c-Src tyrosine kinases was performed using NAMD 2.9 package and CHARMM 27 force field.

In molecular dynamics, successive configurations of the system are generated by integrating Newton's law of motion. The result is a trajectory that specifies how the positions and velocities of the particles in the system vary with time. The trajectory is obtained by solving the differential equations embodied in Newton's second law ($F = ma$).[30]

$$\frac{d^2x_i}{dt^2} = \frac{F_{x_i}}{m_i} \quad (2.1)$$

This equation describes the motion of a particle of mass m_i along one coordinate(x_i). F_{x_i} is the force exerted on the particle in that direction. Through this equation, we can find the trajectory of how the velocity and position of particles in the system change over time.

1.1. Molecular mechanic force field

In order to perform simulation, a potential function called a *force field* must be defined in the following relationship.

$$F = -\frac{dU}{dr} \quad (2.2)$$

Most molecular modeling force fields today are interpreted as four elements bond stretching, angle bending, bond rotation (torsion) and non-bonded interaction, as shown in the following figure (Fig. 2-1). The three components except non-bonded

interaction corresponds to bonded-part of potential function. These four components are associated with the "deviation" for bonds and angles from their reference or equilibrium values.

$$\begin{aligned}
 U(r^N) = & \sum_{bonds} \frac{k_i}{2} (l_i - l_{i,0})^2 + \sum_{angles} \frac{k_i}{2} (\theta_i - \theta_{i,0})^2 \\
 & + \sum_{torsions} \frac{V_n}{2} (1 + \cos(n\omega - \gamma)) \\
 & + \sum_{i=1}^N \sum_{j=i+1}^N \left(4\epsilon_{ij} \left[\left(\frac{\sigma_{ij}}{r_{ij}} \right)^{12} - \left(\frac{\sigma_{ij}}{r_{ij}} \right)^6 \right] + \frac{q_i q_j}{4\pi\epsilon_0 r_{ij}} \right)
 \end{aligned} \tag{2.3}$$

In this formula, $U(r^N)$ is potential energy, and it means the function of position r of N particle. The first term is a formula for the interaction between two bonded atoms, where l_i is the bond length and $l_{i,0}$ is the reference bond length value. The second term gives the value for the angle of the molecule. These items are related to harmonic potential. The third term models dihedral angles, rotation of bond.

The 1st, second, and third term are bonded part in potential function U . The fourth term is a formula for non-bonded interaction. Calculate a pair of atoms (i and j) that are located in different molecules, or that are within the same molecule, but separated by at least three bonds. Non-bonded interactions include Coulomb potential term by electrostatic interactions and Lennard-Jones potential by van der Waals interaction.

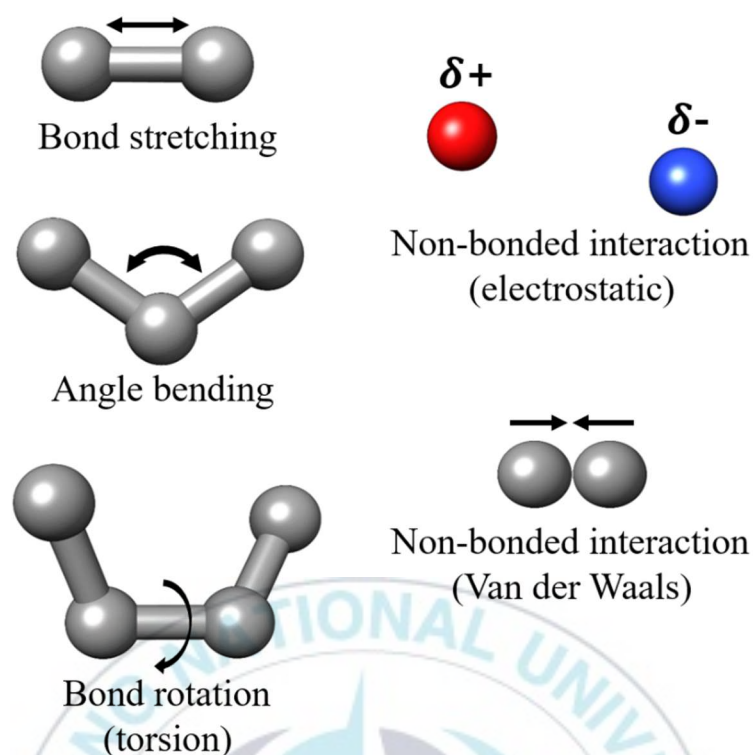


Figure II- 1 . Schematic representation of the four components to a molecular mechanics force field: bond stretching, angle bending, torsional terms and non-bonded interactions.

Bond stretching

Bond stretching refers to the interaction between two bonded atoms. The most basic approach is to use Hooke's law. Morse potential is not commonly used in molecular mechanics force fields. Morse curves cover a wide range from strong equilibrium behavior to dissociation. The energy using Hooke's law varies with the square of the displacement at the reference bond length l_0 .

$$v(l) = \frac{k}{2}(l - l_0)^2 \quad (2.4)$$

The reference bond length l_0 is the value that the bond adopts when all other terms of force field are set to zero.

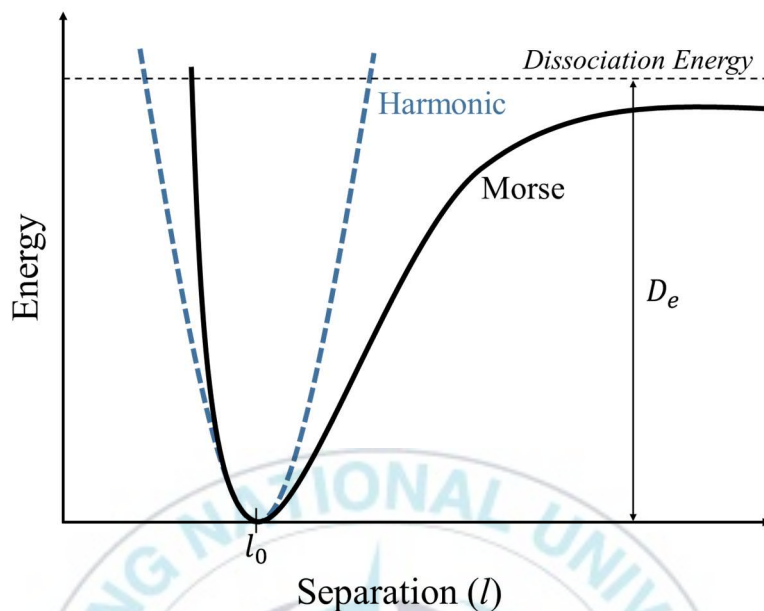


Figure II- 2 . Comparison of the Morse potential (black, solid line) and harmonic oscillator potential (blue, dotted line).

Angle bending

Angle bending provides a value for the angle of the molecule. The angular deviation from the reference value is explained by Hooke's law or harmonic potential.

$$v(\theta) = \frac{k}{2}(\theta - \theta_0)^2 \quad (2.5)$$

The contribution of each angle is specified by force constant and reference value.

Bond rotation

Bond rotation is a value modified from the reference values of bond stretching and angle bending. Therefore, considerable energy is required. The following is the equation for the potential of bond rotation.

$$v(\omega) = \sum_{n=0}^N \frac{V_n}{2} [1 + \cos(n\omega - \gamma)] \quad (2.6)$$

In this formula, V_n is the torsion force constant and n is the multiplicity of function. This value means the minimum value when the bond rotates 360° . ω is the *dihedral angle*, and γ is the *phase factor* indicating the position when the torsion angle is the minimum.

Non-bonded interaction

Non-bonded interactions provide information about pairs of atoms (i and j) that are located in different molecules, or that exist within the same molecule but are separated by three or more bonds. Non-bonded interaction involves two forces, first looking at electrostatic interactions. The electrostatic interactions between two molecules or nonadjacent atoms in the same molecule are obtained as the sum of the interactions between point charges.

$$v = \sum_{i=1}^{N_A} \sum_{j=1}^{N_B} \frac{q_i q_j}{4\pi\epsilon_0 r_{ij}} \quad (2.7)$$

In this formula, N_A and N_B mean the number of point charges of the molecule. Another force of non-bonded interaction is van der Waals interaction. Unlike electrostatic interactions, van der Waals interaction consists of non-bonding

interactions between all atoms, and this formula is expressed as Lennard-Jones potential.

$$v(r_{ij}) = \sum_{i=1}^N \sum_{j=i+1}^N 4\epsilon_{ij} \left[\left(\frac{\sigma_{ij}}{r_{ij}} \right)^{12} - \left(\frac{\sigma_{ij}}{r_{ij}} \right)^6 \right] \quad (2.8)$$

In this formula, r_{ij} means the distance between atoms i and j , and ϵ means the energy depth indicating the bonding of particles. σ_{ij} means collision diameter between atoms i and j , and the separation energy after collision is 0. Looking at the difference between r^{-12} and r^{-6} , r^{-12} means strong repulsion at short distances due to overlap of electron orbitals, and r^{-6} at long distances. It refers to the weak attraction between individual molecules. Therefore, when the distance between two particles approaches 0, it converges to infinity.

Particle Mesh Ewald (PME)

When performing calculations in the system, long-range interactions should be considered. Particle Mesh Ewald (PME) is one of the calculation methods to apply long-range interactions in systems with periodic boundary conditions.[31, 32]

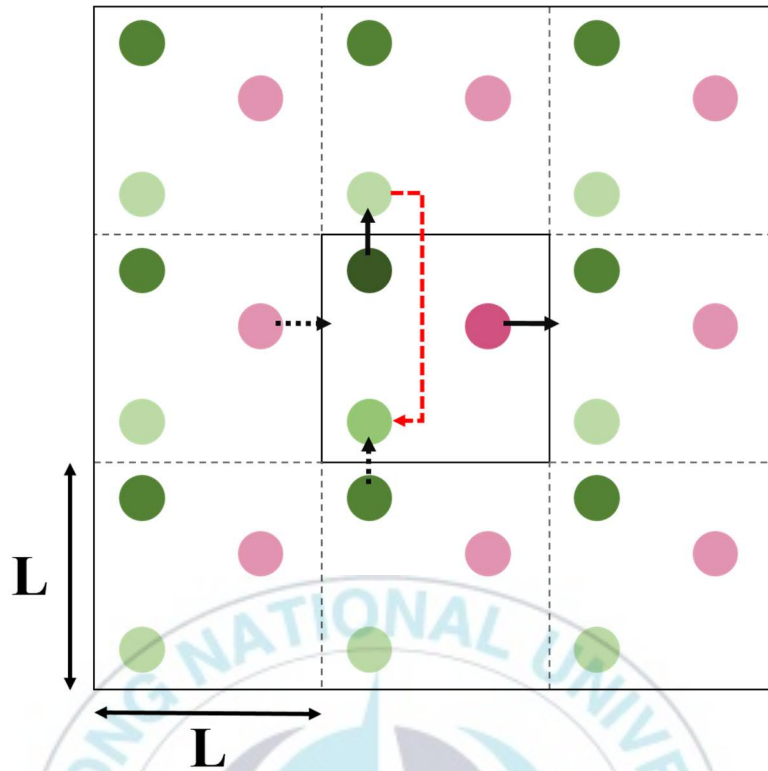


Figure II- 3 . Periodic boundary conditions in two dimensions. The length of box is L.

To understand this calculation, we envision a system with charged particles, both positive and negative. At this time, the system is electrically neutral ($\sum_i q_i = 0$). The system has a periodic boundary condition as shown in (Fig . II-3), and charged particles are located in a cube with a diameter of L. When performing simulation, the number of cubes is said to be N. The particles located inside the Cube repel each other at a short distance. Under these conditions, the coulomb potential energy is:

$$u_{coul} = \frac{1}{2} \sum_{i=1}^N q_i \phi(r_i) \quad (2.9)$$

In this formula, $\phi(r_i)$ means the electrostatic potential at the position of ion i .

$$\phi(r_i) = \sum'_{j,n} \frac{q_j}{|\mathbf{r}_{ij} + \mathbf{n}L|} \quad (2.10)$$

Where the prime on the summation indicates that the sum is over all periodic images n and over all particles j , except $j = i$ if $n = 0$. \mathbf{r}_{ij} is the minimum distance between i and j .

In addition, we assume that the compensating charge distribution surrounding an ion i is a Gaussian.

$$\rho_{\text{Gauss}}(r) = -q_i \left(\frac{\alpha}{\pi}\right)^{\frac{3}{2}} \exp(-\alpha r^2) \quad (2.11)$$

α is determined later by considerations of computational efficiency. It satisfies Poisson's equation.

$$-\nabla^2 \phi(\mathbf{r}) = 4\pi\rho(\mathbf{r}) \quad (2.12)$$

We apply the properties of the Poisson equation in Fourier form to compute the electrostatic potential at a point r_i due to a charge distribution $\rho(\mathbf{r})$ that consists of a periodic sum of Gaussians.

$$\rho_1(r) = \sum_{j=1}^N \sum_{\mathbf{n}} q_j \left(\frac{\alpha}{\pi}\right)^{\frac{3}{2}} \exp[-\alpha |\mathbf{r} - (\mathbf{r}_j + \mathbf{n}L)|^2] \quad (2.13)$$

The electrostatic potential in a Fourier transform is given as

$$\phi_1(r) = \sum_{k \neq 0} \sum_{j=1}^N \frac{4\pi q_j}{k^2} \exp[i\mathbf{k} \cdot (\mathbf{r}_i - \mathbf{r}_j)] \exp\left(-\frac{k^2}{4\alpha}\right) \quad (2.14)$$

with

$$u_1 = \frac{1}{2V} \sum_{k \neq 0} \frac{4\pi}{k^2} \rho(\mathbf{k})^2 \exp\left(-\frac{k^2}{4\alpha}\right) \quad (2.15)$$

V is the volumes of the system. $\rho(\mathbf{k})$ is Fourier transform of charge distribution.

For the self-interaction to be corrected, u_{self} should be subtracted from the sum of the real-space and Fourier contributions to the Coulomb energy.

$$u_{\text{self}} = \left(\frac{\alpha}{\pi}\right)^{\frac{1}{2}} \sum_{i=1}^N q_i^2 \quad (2.16)$$

Then, electrostatic potential due to a point charge q surrounded by a Gaussian with net charge- q_i is given as

$$\Phi_{\text{short-range}} = \frac{q_i}{r} \text{erfc}(\sqrt{\alpha}r) \quad (2.17)$$

where erfc is complementary error function. The total contribution of the screened Coulomb interactions to the potential energy is then given by

$$u_{\text{short-range}} = \frac{1}{2} \sum_{i \neq j}^N \frac{q_i q_j \text{erfc}(\sqrt{\alpha}r_{ij})}{r_{ij}} \quad (2.18)$$

Finally, the total electrostatic contribution to the potential energy is given by

$$u_{\text{coul}} = \frac{1}{2V} \sum_{k \neq 0} \frac{4\pi}{k^2} |\rho(k)|^2 \exp\left(-\frac{k^2}{4\alpha}\right) - \frac{\left(\frac{\alpha}{\pi}\right)^{\frac{1}{2}}}{2} \sum_{i=1}^N q_i^2 + \frac{1}{2} \sum_{i \neq j}^N \frac{q_i q_j \text{erfc}(\sqrt{\alpha}r_{ij})}{r_{ij}} \quad (2.19)$$

1.2. Targeted Molecular Dynamics Simulation

Targeted molecular dynamics (TMD) simulation is very useful for observing a continuous morphological transition pathway between two known protein types. In TMD simulation, start type '*I*' and target type '*F*' are determined. During the transition from '*I*' to '*F*', each component of the protein is given by a vector, $x = (x_1, \dots, x_{3N})^T$, containing the 3N cartesian coordinates of the position vectors r_1, \dots, r_N of the individual atoms. x_I and x_F are the configurations representing the conformations '*I*' and '*F*'. The distance (ρ) between the configuration of each time step, x , and the target configuration, x_F is given by

$$\rho = |x - x_F| = \left[\sum (x_i - x_{Fi})^2 \right]^{1/2} \quad (2.20)$$

The initial value of ρ is set as the distance between the initial and target structure. During the simulation, ρ is decreased to zero. In this simulation, ρ is used as a control parameter in order to force the system to undergo the desired transition. This is achieved by introducing the constraint.

$$|x - x_F|^2 - \rho^2 = 0 \quad (2.21)$$

Therefore, the TMD simulation must define an external potential, U_{TMD} , to perform the simulation. U_{TMD} is given as

$$U_{TMD} = \frac{k}{2N} [RMSD(t) - RMSD^*(t)]^2 \quad (2.22)$$

N is the number of atom, k is harmonic force constant per atom. $RMSD(t)$ is the Root-Mean-Square Deviation (RMSD) of the simulated structure at time t to the target structure. $RMSD^*(t)$ is the RMSD value at time t that it decrease linearly from the initial to the target structure.

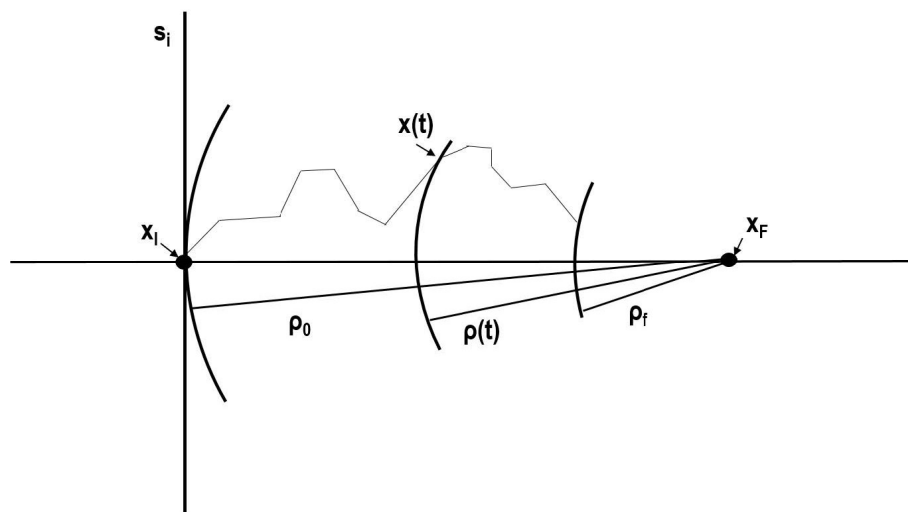


Figure II-4 . Geometry of the conformational transition from \mathbf{x}_i to \mathbf{x}_f . The r -axis is chosen in such a way that the initial configuration defines the origin and the final configuration lies on the positive branch. \mathbf{S}_i is one of the residual Cartesian coordinates. A TMD simulation run generates configuration $\mathbf{x}(\mathbf{t})$ lying on hyperspheres with radius $\rho(\mathbf{t})$ centered in \mathbf{x}_f . The quasicontinuous contraction of the hypersphere from a radius ρ_0 to ρ_f enforces the conformational transition.[33]

2. Molecular docking

Molecular docking aims to predict the protein-ligand complex by calculating the conformation and binding affinity of the ligand in the protein structure. In this study, a protein-ligand structure is formed and compared using a popular docking program, Autodock, and a Swisdock, a web server for blind docking.[25,26, 34]

In this experiment, SWISSDOCK performed docking using a web server and compared the energy. When AUTODOCK 4.2 is executed, 10 docking poses are created using the default docking parameter, and the lowest binding energy is selected to compare the results. Docking results are shown using Discovery Studio.

2.1. Autodock

The ideal docking procedure is a method of searching all degrees of freedom (DOF) in the system by finding the minimum value of the total in the interaction energy between the substrate and the target protein, but has a disadvantage that it takes a very long time. Therefore, Autodock calculates through two methods ; rapid grid-based energy evaluation and efficient search of torsional freedom, to obtain relatively accurate results within a short period of time. The version used in the experiment, AUTODUCK 4.2, calculates the scoring function through the Lamarckian genetic algorithm and the empirical free energy scoring function, and generally provides about 10 docking results. The type of scoring function used here is Force Field-Based Scoring, which is calculated in principle using physical laws, and the result of calculation is derived no matter what docking, but the entropy effect and solvent effect are not considered.[27, 35, 36]

In AUTODUCK, the total docking energy of a given ligand molecule is expressed as the sum of the intermolecular interactions between the ligand complex and the internal steric energy. Using the minimum-energy docked conformation structure, the linear model binding energy is calculated as Gibbs free energy.

$$\Delta G_{bind} = \Delta G_{vdW} + \Delta G_{hb} + \Delta G_{elec} + \Delta G_{solv} + \Delta G_{tor} \quad (2.23)$$

In this formula, vdW means van der Waals, hb is hydrogen bond, elec is electrostatic, solv and tor mean solvation and torsion, respectively. In this formula, the meaning of each Gibbs free energy is as follows.

$$\Delta G_{vdW} = f_{vdW} \sum_{ij} \left(\frac{A_{pq}}{r_{ij}^{12}} - \frac{B_{pq}}{r_{ij}^6} \right) \quad (2.24)$$

$$\Delta G_{hb} = f_{hb} \left[\sum_{ij} E(\theta_{ij}) \left(\frac{C_{pq}}{r_{ij}^{12}} - \frac{D_{pq}}{r_{ij}^{10}} \right) - \sum_i (\Delta G_{p,water}) \right] \quad (2.25)$$

$$\Delta G_{elec} = f_{elec} \sum_{ij} \frac{q_i q_j}{\varepsilon(r_{ij}) r_{ij}} \quad (2.26)$$

The first three terms are vacuo force field energies for intermolecular interaction. A_{pq} and B_{pq} mean Lennard–Jones 12–6 coefficients for non-bonded interactions between atom types p and q, and C_{pq}, D_{pq} is Lennard–Jones 12–10 coefficients for hydrogen bonding between atom types p and q. $E(\theta_{ij})$ is weight dependent upon the angle between i and j, with Columbic electrostatic shielding.

$$\Delta G_{solv} = -f_{solv} \sum_{ij} S_p V_q e^{-r_{ij}^2/2\sigma^2} \quad (2.27)$$

$$\Delta G_{tor} = -f_{tor} N_{tor} \quad (2.28)$$

The following terms refer to the interaction of water and the ligand atom, and the internal steric energy of the ligand molecule related to the torsion of the ligand, respectively.

In the fourth term, $\Delta G_{p,water}$ means free energy change of hydrogen bonding between atom type p and water, S_p and V_q mean solvation parameters atom type p, defined as the volume change of solvating atom type p and atomic volume of atom type q, respectively.

$$\varepsilon(r_{ij}) = F + \frac{H}{l + ke^{-\lambda Hr}} \quad (2.29)$$

Here, $H = e_0 - F$ (e_0 is relative dielectric constant of water at 25 °C = 78.4 (694 pF/m)) and F , l and k are sigmoidal parameters of -8.5525 , 0.003627 , and 7.7839 respectively.[35]

All the terms in this free energy function have been described previously. A combination of a force field with linear weights is used as a free energy function.

2.2. Swissdock

Swissdock, which provides blind docking, is a web-based docking service (<http://www.swissdock.ch>) that shows docking to small molecules of the target protein. Based on the EADock DSS engine, Swissdock combines a setup script to prepare the target protein and ligand input file. In addition, an efficient Ajax/HTML interface is designed and implemented so that users can easily obtain desired docking results. The binding mode with the most favorable energy is evaluated and clustered with FACTS (fast analytical continuum treatment of solvation), and the most favorable cluster can be visualized online and downloaded to the computer.[37]

III. Results and Discussion

When investigating the binding of a protein to a drug, we mainly study the protein with a fixed form, but the actual protein constantly changes form in the body. In this case, in order to obtain a more accurate study of the result of the interaction between the protein and the drug, the morphological change of the protein was implemented by Molecular Simulation. And subsequently docking was performed on the result to compare the results.

Targeted Molecular Dynamics

The trajectory for 10 ns was investigated using Targeted Molecular Simulation. Snapshots of the intermediate process of the structural change from the inactive state to the active state were selected at 2 ns intervals, respectively. In this study, all six structures were used for imatinib and docking.

Protein label	Time	
Protein A	0ns	Inactive state : PDB(2SRC) : Initial
Protein B	2ns	Generated by targeted MD simulation
Protein C	4ns	Generated by targeted MD simulation
Protein D	6ns	Generated by targeted MD simulation
Protein E	8ns	Generated by targeted MD simulation
Protein F	10ns	Active state : PDB(1Y75) : Target

Table III- 1 . Labels for the various different conformations of c-Src tyrosine kinase generated by targeted MD simulation.

Structures selected for analysis are inactive protein structure (A) and intermediate structures selected at 2 ns intervals; protein structure (B) corresponding to 2 ns, protein structure (C) corresponding to 4 ns, and protein

corresponding to 6 ns It is a structure (D), a protein structure (E) corresponding to 8 ns, and a protein structure (F) corresponding to 10 ns. In particular, the protein structure (F) corresponding to the last purpose is exactly in accordance with the active state protein crystal structure. (Table 3_1 and Fig3_1)

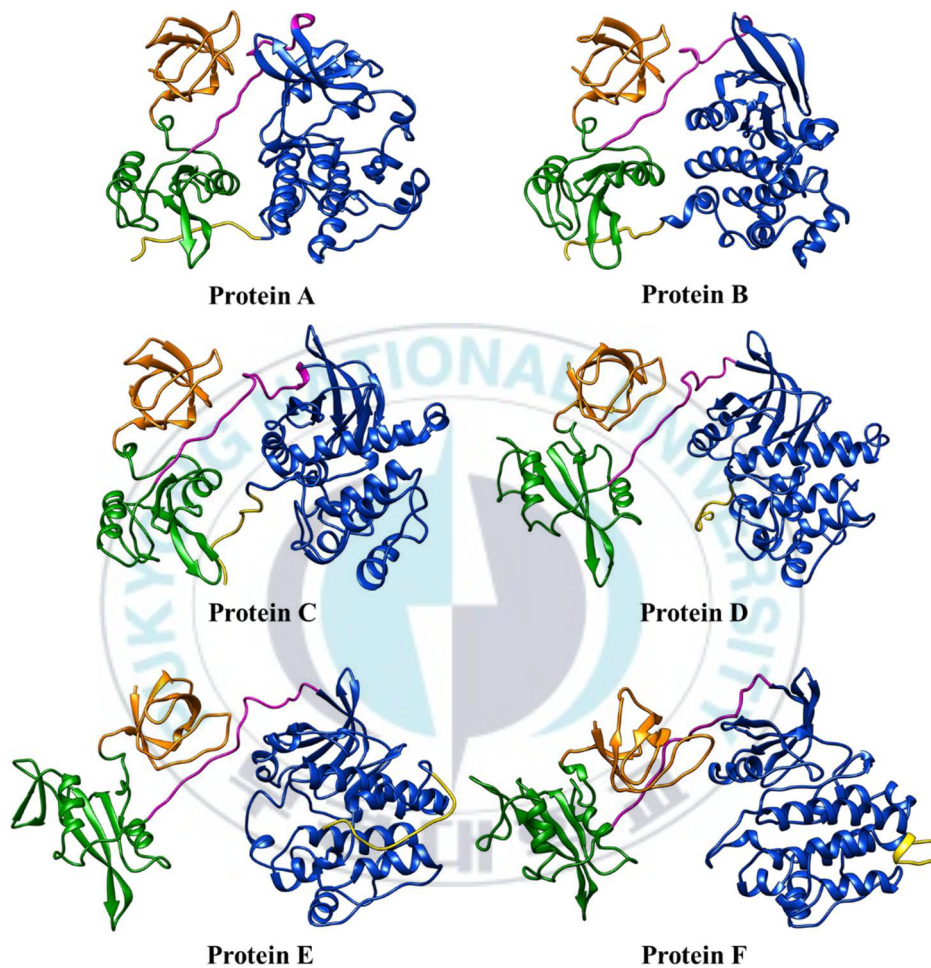


Figure III- 1 . Six Snapshots of TMD trajectory during 10 ns. (A) 0ns : Starting structure (Inactive conformation). (B) 2 ns, (C) 4 ns, (D) 6 ns, (E) 8 ns, (F) 10 ns : Targeting structure (Active conformation). In particular, the protein structure (F) exactly matches the active state protein crystal structure.

Docking Result

Two different software was used (SWISSDOCK, AUTODOCK4.2) to dock imatinib to the structure of six c-Src proteins identified in the MD simulation. The following are docking results.

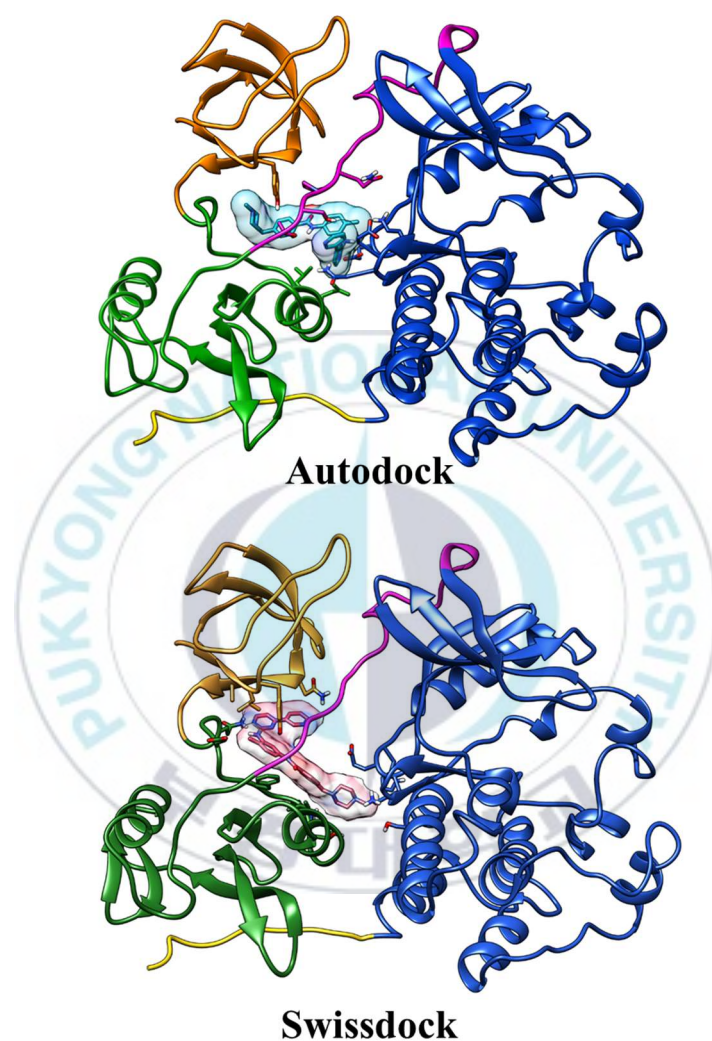


Figure III- 2 . At this time, Imatinib moves dynamically without being fixed according to a given torsion when it is docked. The gridbox of Autodock is set to (60*60*60Å³).

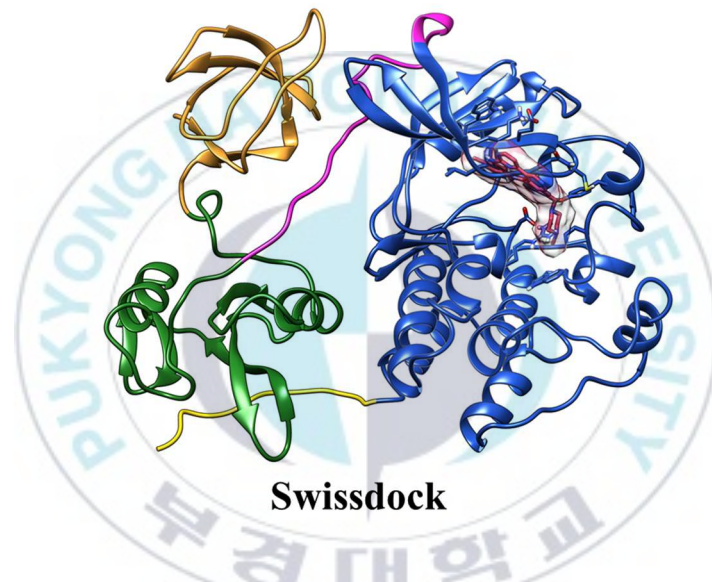
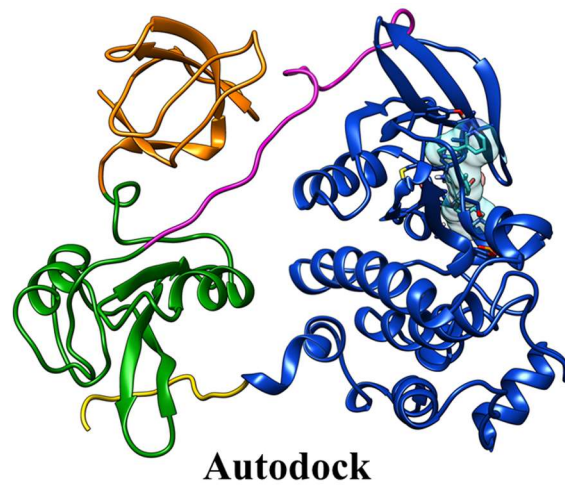
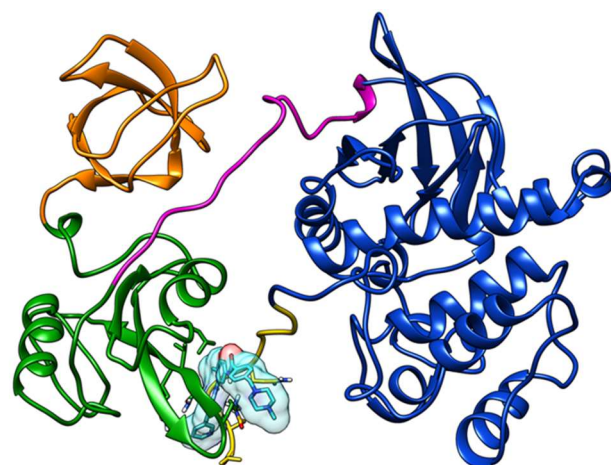
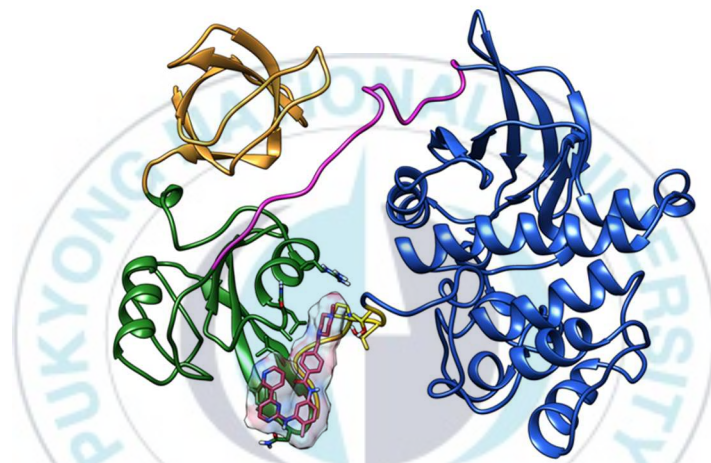


Figure III- 3 . 2ns structure created by MD simulation. Docking images of Imatinib to a c-Src tyrosine kinase are generated by AUTODOCK (blue) and SWISSDOCK (pink)

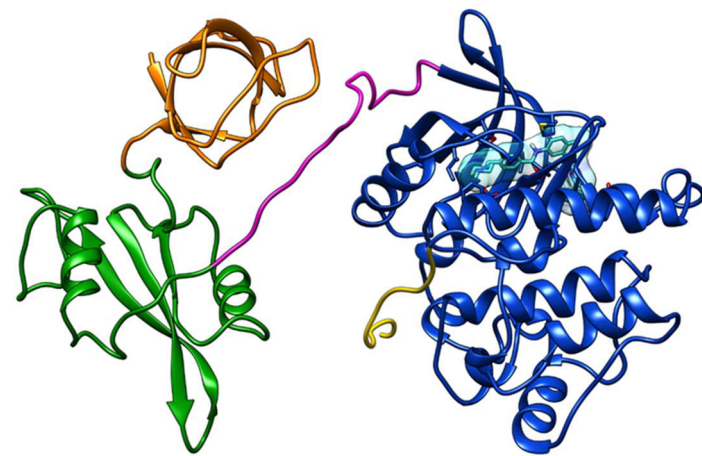


Autodock

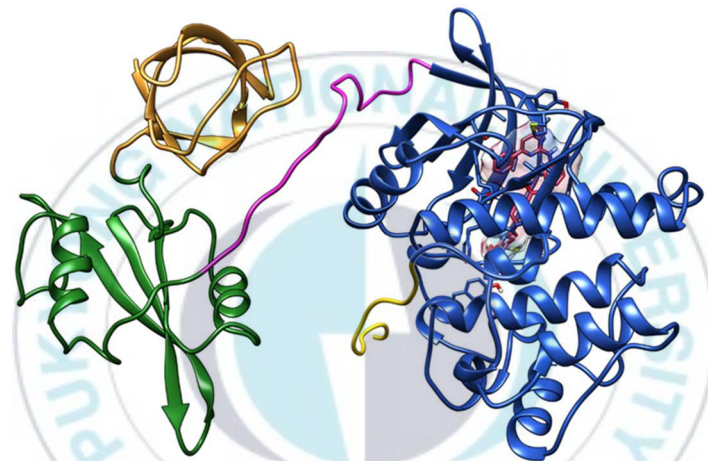


Swissdock

Figure III- 4 . 4ns structure created by MD simulation. Docking images of Imatinib to a c-Src tyrosine kinase are generated by AUTODOCK (blue) and SWISSDOCK (pink)

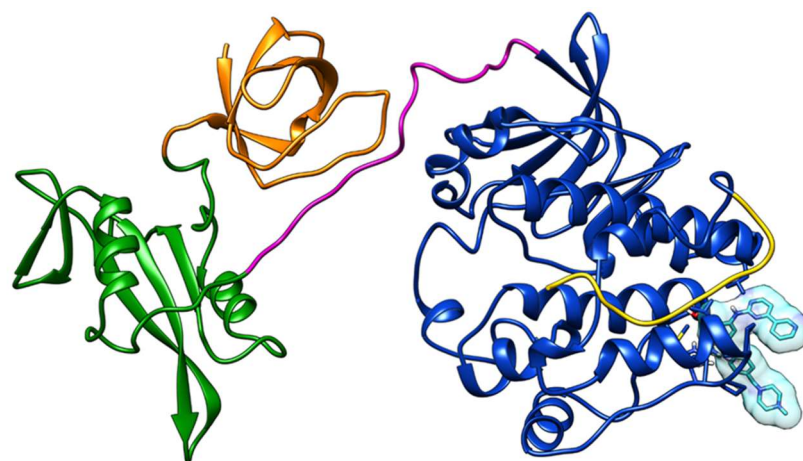


Autodock

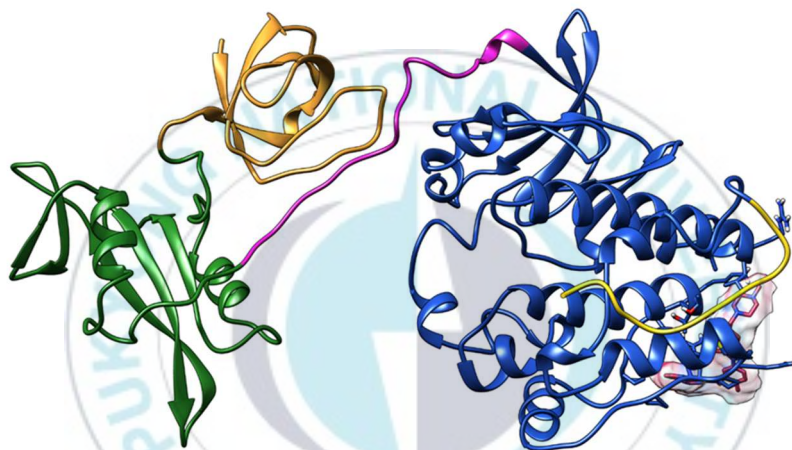


Swissdock

Figure III- 5 . 6ns structure created by MD simulation. Docking images of Imatinib to a c-Src tyrosine kinase are generated by AUTODOCK (blue) and SWISSDOCK (pink).

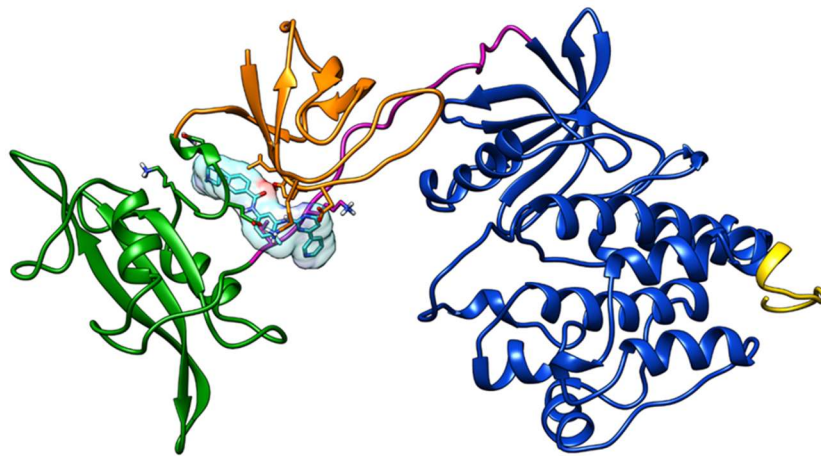


Autodock

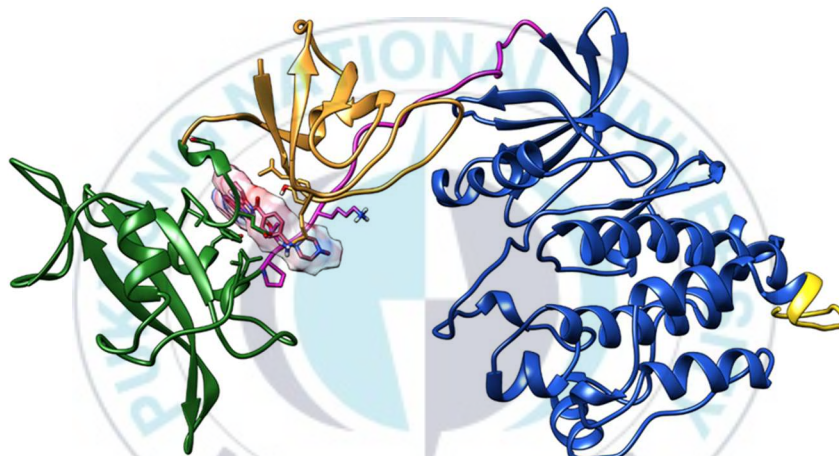


Swissdock

Figure III- 6 . 8ns structure created by MD simulation. Docking images of Imatinib to a c-Src tyrosine kinase are generated by AUTODOCK (blue) and SWISSDOCK (pink).



Autodock



Swissdock

Figure III- 7 . 10ns structure created by MD simulation. Docking images of Imatinib to a c-Src tyrosine kinase are generated by AUTODOCK (blue) and SWISSDOCK (pink).

At this time, Imatinib moves dynamically without being fixed according to a given torsion when it is docked. The size of gridbox of AUTODOCK is set to (60*60*60 Å³). Imatinib binds to different parts of c-Src tyrosine kinase at different time states.

In the docking results, the docking structure between each protein and imatinib was selected as the structure that took the highest among each scoring function. In the above results, the protein structures B, D, and E show that imatinib binds to the kinase region (blue region) of c-Src tyrosine kinase. On the other hand, in the case of protein F, that is, when the protein is fully activated, it shows that imatinib binds to the linker region (pink portion) rather than the kinase region of c-Src tyrosine kinase. The results show a very consistent trend in both the SWISSDOCK and AUTODOCK cases.

The results of Gibbs Free Energy calculated based on the most superior scoring function for molecular docking are expressed graphically.

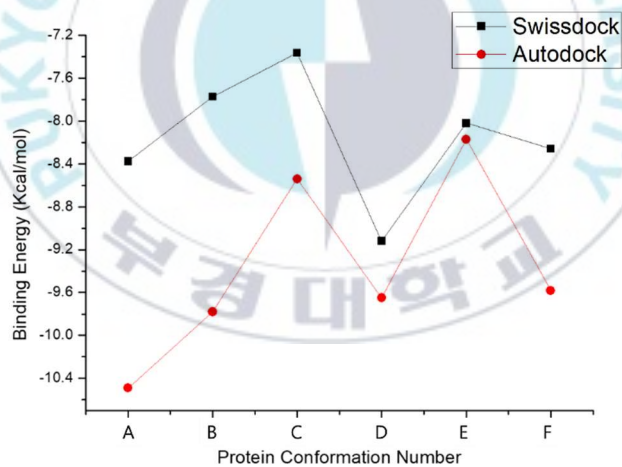


Figure III- 8 . Gibbs Free Energy for binding of imatinib to various c-Src tyrosine kinase conformations. The arrow denotes the most stable conformation of c-Src tyrosine kinase binding to imatinib.

For a total of six different protein structures, the lowest Gibbs energy value resulted in the binding of SWISSDOCK to the protein structure “D” (-9.2 kcal/mol), whereas in the case of AUTODOCK it was completely inactive. Protein structure appeared as structure “A” (-10.6 kcal/mol).

A careful investigation of AUTODOCK results shows that imatinib binds to the linker region rather than the kinase region of the c-Src tyrosine kinase protein structure “A”. According to X-ray studies, the binding of c-Src tyrosine kinase protein to imatinib is known to occur in an inactive state expressed as “DFG-out”. [23]

According to these results, the binding site of imatinib that binds to the protein structure “A”. AUTODOCK is somewhat different from the X-ray structure. As shown in Figure 3-8, it can be seen from the results of both SWISSDOCK and AUTODOCK that a protein structure with a very stable Gibbs free energy value exists. (Indicated by arrows in Fig. III-8). Interesting results show that imatinib binding near DFG (Asp(404)-Phe(405)-Gly(406)) shows that the protein “D” structure of the six protein structures is very similar to the X-ray results (Fig III-9).

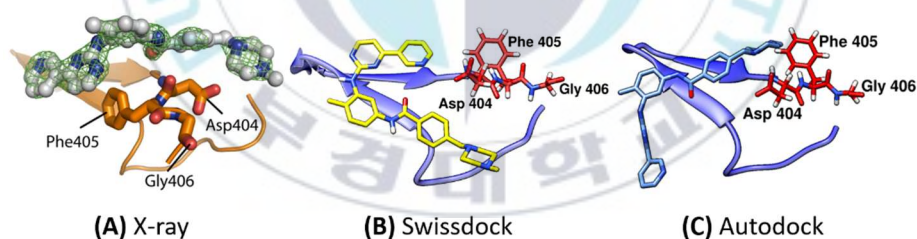


Figure III-9. Relative conformation of imatinib with DFG (Asp(404)-Phe(405)-Gly(406)) conformation of c-Src tyrosine kinase generated by (A) X-ray (B) SWISSDOCK (C) AUTODOCK.

The arrangement of imatinib in SWISSDOCK (Fig. III-9,(B)) and AUTODOCK (Fig. III-9,(C)) was compared with the X-ray structure (Fig. III-9,(A)). For the alignment and binding sites of imatinib, the X-ray structure and the molecular docking structure do not completely match, but the c-Src tyrosine kinase involved in the binding was generated through molecular dynamics simulation

IV. Conclusions

The protein state to which imatinib binds with a relatively low binding energy is not a complete inactive state, but an intermediate protein structure from inactive to active. In the process of c-Src tyrosine kinase structure change, it was found that a specific structure to which imatinib binds more strongly exists. As a result, in the development of drugs targeting allosteric proteins that cause structural changes, in addition to those in the “start” state (inactive state) and “final” state (active state) of the structural change, the “middle” stage of the structural change This means that protein structure must also be considered. The results of this study strongly support the drug 'residence time model'[38], in which the conformational dynamics of the protein targeted for the drug has a very important effect on the binding and dissociation of the drug. The study of c-Src tyrosine kinase structure change and binding of imatinib was conducted, and c-Src tyrosine kinase structure change process was observed.

In the process of structural change, the binding with the strongest imatinib corresponding to a specific time was confirmed, which is a common result of two programs, AUTODOCK and SWISSDOCK, which have different scoring functions.

Reference

- [1] Manning, G., Whyte, D. B., Martinez, R., Hunter, T., & Sudarsanam, S. (2002). The protein kinase complement of the human genome. *Science*, 298(5600), 1912-1934.
- [2] Schlessinger, J. (2000). Cell signaling by receptor tyrosine kinases. *Cell*, 103(2), 211-225.
- [3] Salmeen, A., Andersen, J. N., Myers, M. P., Meng, T. C., Hinks, J. A., Tonks, N. K., & Barford, D. (2003). Redox regulation of protein tyrosine phosphatase 1B involves a sulphenyl-amide intermediate. *Nature*, 423(6941), 769-773.
- [4] Hubbard, S. R., & Till, J. H. (2000). Protein tyrosine kinase structure and function. *Annual review of biochemistry*, 69(1), 373-398.
- [5] Bhullar, K. S., Lagarón, N. O., McGowan, E. M., Parmar, I., Jha, A., Hubbard, B. P., & Rupasinghe, H. V. (2018). Kinase-targeted cancer therapies: progress, challenges and future directions. *Molecular cancer*, 17(1), 1-20.
- [6] Weinberg, R. A., & Weinberg, R. A. (2013). *The biology of cancer*. Garland science.
- [7] Gocek, E., Moulas, A. N., & Studzinski, G. P. (2014). Non-receptor protein tyrosine kinases signaling pathways in normal and cancer cells. *Critical reviews in clinical laboratory sciences*, 51(3), 125-137.
- [8] Thomas, S. M., & Brugge, J. S. (1997). Cellular functions regulated by Src family kinases. *Annual review of cell and developmental biology*, 13(1), 513-609.
- [9] Sicheri, F., & Kuriyan, J. (1997). Structures of Src-family tyrosine kinases. *Current opinion in structural biology*, 7(6), 777-785.
- [10] Rous, P. (1911). A sarcoma of the fowl transmissible by an agent separable from the tumor cells. *The Journal of experimental medicine*, 13(4), 397.
- [11] Matsouka, P. T., & Flier, J. S. (1989). Relationship between c-src tyrosine kinase activity and the control of glucose transporter gene

- expression. *Molecular endocrinology*, 3(11), 1845-1851.
- [12] Roskoski Jr, R. (2004). Src protein-tyrosine kinase structure and regulation. *Biochemical and biophysical research communications*, 324(4), 1155-1164.
- [13] Xu, W., Doshi, A., Lei, M., Eck, M. J., & Harrison, S. C. (1999). Crystal structures of c-Src reveal features of its autoinhibitory mechanism. *Molecular cell*, 3(5), 629-638
- [14] Paul, M. K., & Mukhopadhyay, A. K. (2004). Tyrosine kinase-role and significance in cancer. *International journal of medical sciences*, 1(2), 101.
- [15] Yoon, H. J., Lee, S., Park, S. J., & Wu, S. (2018). Network approach of the conformational change of c-Src, a tyrosine kinase, by molecular dynamics simulation. *Scientific reports*, 8(1), 1-10.
- [16] Chong, Y. P., Ia, K. K., Mulhern, T. D., & Cheng, H. C. (2005). Endogenous and synthetic inhibitors of the Src-family protein tyrosine kinases. *Biochimica et Biophysica Acta (BBA)-Proteins and Proteomics*, 1754(1-2), 210-220.
- [17] Pérez, Y., Maffei, M., Igea, A., Amata, I., Gairí, M., Nebreda, A. R., ... & Pons, M. (2013). Lipid binding by the Unique and SH3 domains of c-Src suggests a new regulatory mechanism. *Scientific reports*, 3, 1295.
- [18] Young, M. A., Gonfloni, S., Superti-Furga, G., Roux, B., & Kuriyan, J. (2001). Dynamic coupling between the SH2 and SH3 domains of c-Src and Hck underlies their inactivation by C-terminal tyrosine phosphorylation. *Cell*, 105(1), 115-126.
- [19] Moroco, J. A., Craigo, J. K., Iacob, R. E., Wales, T. E., Engen, J. R., & Smithgall, T. E. (2014). Differential sensitivity of Src-family kinases to activation by SH3 domain displacement. *PloS one*, 9(8), e105629.
- [20] Roskoski Jr, R. (2015). Src protein-tyrosine kinase structure, mechanism, and small molecule inhibitors. *Pharmacological research*, 94, 9-25.
- [21] Cowan-Jacob, S. W., Fendrich, G., Manley, P. W., Jahnke, W., Fabbro, D., Liebetanz, J., & Meyer, T. (2005). The crystal structure of a c-Src complex in an active conformation suggests possible steps in c-Src

- activation. *Structure*, 13(6), 861-871.
- [22] Blume-Jensen, P., & Hunter, T. (2001). Oncogenic kinase signalling. *Nature*, 411(6835), 355-365.
- [23] Seeliger, M. A., Nagar, B., Frank, F., Cao, X., Henderson, M. N., & Kuriyan, J. (2007). c-Src binds to the cancer drug imatinib with an inactive Abl/c-Kit conformation and a distributed thermodynamic penalty. *Structure*, 15(3), 299-311.
- [24] Wu, P., Nielsen, T. E., & Clausen, M. H. (2016). Small-molecule kinase inhibitors: an analysis of FDA-approved drugs. *Drug discovery today*, 21(1), 5-10.
- [25] Meng, X. Y., Zhang, H. X., Mezei, M., & Cui, M. (2011). Molecular docking: a powerful approach for structure-based drug discovery. *Current computer-aided drug design*, 7(2), 146-157.
- [26] Wang, R., Lu, Y., & Wang, S. (2003). Comparative evaluation of 11 scoring functions for molecular docking. *Journal of medicinal chemistry*, 46(12), 2287-2303.
- [27] Morris, G. M., Huey, R., Lindstrom, W., Sanner, M. F., Belew, R. K., Goodsell, D. S., & Olson, A. J. (2009). AutoDock4 and AutoDockTools4: Automated docking with selective receptor flexibility. *Journal of computational chemistry*, 30(16), 2785-2791.
- [28] Pagadala, N. S., Syed, K., & Tuszynski, J. (2017). Software for molecular docking: a review. *Biophysical reviews*, 9(2), 91-102.
- [29] Schlitter, J., Engels, M., Krüger, P., Jacoby, E., & Wollmer, A. (1993). Targeted molecular dynamics simulation of conformational change-application to the T \leftrightarrow R transition in insulin. *Molecular Simulation*, 10(2-6), 291-308.
- [30] Phillips, J. C., Braun, R., Wang, W., Gumbart, J., Tajkhorshid, E., Villa, E., ... & Schulten, K. (2005). Scalable molecular dynamics with NAMD. *Journal of computational chemistry*, 26(16), 1781-1802.
- [31] Frenkel, D., & Smit, B. (2001). *Understanding molecular simulation: from algorithms to applications* (Vol. 1). Elsevier.

- [32] Darden, T., York, D., & Pedersen, L. (1993). Particle mesh Ewald: An $N \cdot \log(N)$ method for Ewald sums in large systems. *The Journal of chemical physics*, 98(12), 10089-10092.
- [33] Schlitter, J., Engels, M., & Krüger, P. (1994). Targeted molecular dynamics: a new approach for searching pathways of conformational transitions. *Journal of molecular graphics*, 12(2), 84-89.
- [34] Forli, S., Huey, R., Pique, M. E., Sanner, M. F., Goodsell, D. S., & Olson, A. J. (2016). Computational protein–ligand docking and virtual drug screening with the AutoDock suite. *Nature protocols*, 11(5), 905-919.
- [35] Hill, A. D., & Reilly, P. J. (2015). Scoring functions for AutoDock. In *Glycoinformatics* (pp. 467-474). Humana Press, New York, NY.
- [36] Morris, G. M., Goodsell, D. S., Halliday, R. S., Huey, R., Hart, W. E., Belew, R. K., & Olson, A. J. (1998). Automated docking using a Lamarckian genetic algorithm and an empirical binding free energy function. *Journal of computational chemistry*, 19(14), 1639-1662.
- [37] Grosdidier, A., Zoete, V., & Michielin, O. (2011). SwissDock, a protein-small molecule docking web service based on EADock DSS. *Nucleic acids research*, 39(suppl_2), W270-W277.
- [38] Copeland, R. A. (2016). The drug–target residence time model: a 10-year retrospective. *Nature Reviews Drug Discovery*, 15(2), 87.

Acknowledgement

짧게만 느껴지는 2년이 흘러 석사 졸업을 앞두고 있습니다. 2년전, 대학원 진학을 앞두고 약간의 두려움이 있었지만, 많은 분들의 응원과 도움 덕분에 부족한 제가 조금이나마 성장할 수 있는 너무나도 의미 있는 시간이었습니다.

2년 동안 저를 격려해 주시고 많은 가르침을 주신 우상욱 지도교수님께 감사드립니다. 혼란스러워하는 저를 올바른 방향으로 이끌어 주신 교수님의 지도 덕분에 많은 것을 배울 수 있었고, 성장 할 수 있었습니다. 다시 한번 감사드립니다. 바쁘신 와중에도 논문이 잘 완성될 수 있도록 지도해 주신 남승일 교수님과 홍지상 교수님께 감사드립니다.

대학원 생활 동안 많은 일이 있었지만, 교수님, 선배들, 친구들 가족들의 응원과 격려 덕분에 즐거운 대학원 생활을 할 수 있었습니다. 언제나 저를 응원해 주신 수진 언니와 함께 생활하며 조언을 아끼지 않은 실험실의 이상원 선생님과 KUNDU 박사님께도 감사를 포함합니다. 마지막으로 늘 저의 든든한 버팀목이 되어주신 존경하는 부모님과 사랑하는 동생들에게도 감사합니다.

이 논문이 완성되기까지 도움을 주신 모든 분들에게 다시 한번 감사 드리며, 늘 행복한 일만 가득 하셨으면 합니다.

2020년 8월

박수현